



# Stabilization of the Simplest Criegee Intermediate from the Reaction between Ozone and Ethylene: A High-Level Quantum Chemical and Kinetic Analysis of Ozonolysis

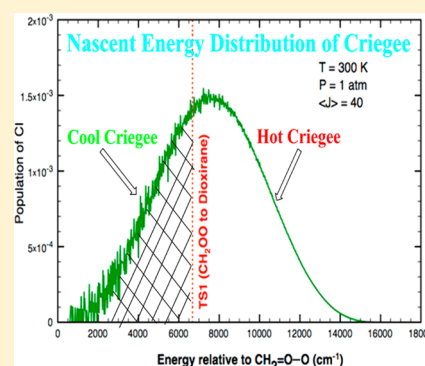
Thanh Lam Nguyen,<sup>†</sup> Hyunwoo Lee,<sup>†</sup> Devin A. Matthews,<sup>†</sup> Michael C. McCarthy,<sup>‡</sup> and John F. Stanton<sup>\*,†</sup>

<sup>†</sup>Department of Chemistry, The University of Texas at Austin, Mail Stop A5300, Austin, Texas 78712-0165, United States

<sup>‡</sup>Harvard-Smithsonian Center for Astrophysics, 60 Garden Street, Cambridge, Massachusetts 02138, United States

## S Supporting Information

**ABSTRACT:** The fraction of the collisionally stabilized Criegee species  $\text{CH}_2\text{OO}$  produced from the ozonolysis of ethylene is calculated using a two-dimensional ( $E$ ,  $J$ )-grained master equation technique and semiclassical transition-state theory based on the potential energy surface obtained from high-accuracy quantum chemical calculations. Our calculated yield of  $42 \pm 6\%$  for the stabilized  $\text{CH}_2\text{OO}$  agrees well, within experimental error, with available (indirect) experimental results. Inclusion of angular momentum in the master equation is found to play an essential role in bringing the theoretical results into agreement with the experiment. Additionally, yields of HO and  $\text{HO}_2$  radical products are predicted to be  $13 \pm 6\%$  and  $17 \pm 6\%$ , respectively. In the kinetic simulation, the HO radical product is produced mostly from the stepwise decomposition mechanism of primary ozonide rather than from dissociation of hot  $\text{CH}_2\text{OO}$ .



## INTRODUCTION

Criegee intermediates (CIs) are reactive species known to be produced from ozonolyses of alkenes.<sup>1,2</sup> These species are believed to play important roles in the atmosphere, where they are thought to be involved in the production of hydroxyl radicals, hydroperoxy radicals, and relatively unvolatile organic compounds.<sup>3–8</sup> The chemistry of “hot” and “cool” Criegee species is expected to be very different; “hot” CIs with high internal energy are believed to dissociate quickly to yield HO/ $\text{HO}_2$  radicals (e.g.,  $\text{HO}_2$  is produced from secondary chemical reactions of H or HCO or  $\text{RCH}_2\text{O}$  radical products with  $\text{O}_2$ ) or to convert to acids or esters, which both undergo subsequent chemistry. In contrast, “cool” CIs (or stabilized Criegees designated as SCI), which have a longer lifetime, are assumed to carry out atmospherically significant bimolecular reactions (with water, carbonyls,  $\text{SO}_2$ , or  $\text{NO}_2$ , and so on) and to participate in the formation of aerosols as well as acid rain (e.g.,  $\text{H}_2\text{SO}_4$ ).<sup>3–9</sup>

SCIs produced from ozonolysis of alkenes have never been observed directly,<sup>10–18</sup> but are believed to be present where formation of secondary ozonides (SOZ) or other compounds (e.g.,  $\text{H}_2\text{SO}_4$  from CI +  $\text{SO}_2/\text{H}_2\text{O}$  or carbonyls from CIs +  $\text{H}_2\text{O}$ ) have been (indirectly) detected using scavengers (such as  $\text{CH}_2\text{O}$ ,  $\text{CH}_3\text{CHO}$ ,  $\text{H}_2\text{O}$ ,  $\text{SO}_2$ ,  $\text{HC}(\text{O})\text{OH}$ , or others).<sup>19–30</sup> Very recently, several small Criegees (i.e.,  $\text{H}_2\text{COO}$ ,  $\text{H}_3\text{CCHOO}$ ,  $(\text{CH}_3)_2\text{COO}$ , and  $\text{C}_2\text{H}_5\text{CHOO}$ ) have been observed spectroscopically in the laboratory using different kinds of reactions and various techniques.<sup>11–18</sup> This work has produced “cool” Criegees with a sufficiently low internal energy so that they have a lifetime that is sufficient for detection and therefore opens new avenues

for studies of spectroscopy, thermochemistry, reactivity, and chemical kinetics of Criegees. In the atmosphere, Criegees are mainly produced from ozonolyses of alkenes (or their derivatives).<sup>3–9</sup> Rationally, it is expected that some fraction of vibrationally excited Criegee may be collisionally stabilized under tropospheric conditions ( $T \approx 220\text{--}308\text{ K}$  and  $P \approx 0.25\text{--}1\text{ atm}$ ).<sup>3</sup> Given that Criegees are thought to play important roles (such as formation of photochemical smog and global climate change) in the troposphere, it is important to explore the mysteries of Criegee chemistry. In particular, we will address two challenging questions, namely, (i) what fraction of stabilized Criegee  $\text{CH}_2\text{OO}$  is produced from  $\text{O}_3 + \text{C}_2\text{H}_4$  and (ii) why has stabilized Criegee  $\text{CH}_2\text{OO}$  produced from  $\text{O}_3 + \text{C}_2\text{H}_4$  not yet been observed *directly* in the laboratory? By using a scavenger to trap stabilized  $\text{CH}_2\text{OO}$ , the fraction of SCI was determined experimentally to vary from 0.35 to 0.55, depending on scavengers and reaction conditions used (see Table 1).<sup>19–30</sup> On the theoretical side, although the reaction of  $\text{O}_3$  with  $\text{C}_2\text{H}_4$  has been studied extensively,<sup>31–37</sup> in terms of kinetics there is only the theoretical work of Olzmann et al.<sup>36</sup> who computed the fraction of stabilized  $\text{CH}_2\text{OO}$  using a one-dimensional master-equation technique and the potential energy surface obtained with density functional theory (DFT) and CCSD(T) methods.<sup>37</sup> In that work,<sup>36</sup> the fraction of SCI was predicted to be about 0.25, roughly half that which has been inferred from experiments (see Table 1).

**Received:** March 3, 2015

**Revised:** May 5, 2015

**Published:** May 6, 2015



**Table 1. Yield of Collisional Stabilized Criegee Intermediate ( $Y_{\text{SCI}}$ ) from the  $\text{O}_3 + \text{C}_2\text{H}_4$  Reaction**

$Y_{\text{SCI}}$	conditions ( $T, P$ )	SCI scavenger	reference
$0.48 \pm 0.05$	300 K and 1 atm	n/a; theory	this work
0.21 to 0.29	298 K and 1 atm	n/a; theory	Olzmann et al., <sup>36</sup> 1997
$0.54 \pm 0.12$	298 K and 1 atm	CO	Alam et al., <sup>28</sup> 2011
$0.39 \pm 0.11$	298 K and 1 atm	$\text{H}_2\text{O}, \text{HC(O)OH}$	Hasson et al., <sup>27</sup> 2001
0.49–0.55	295 $\pm$ 2 K and 730 $\pm$ 3 Torr	$\text{CF}_3\text{C(O)CF}_3$ , $\text{CH}_3\text{CHO}$	Horie et al., <sup>26</sup> 1999
0.50	296 $\pm$ 2 K and 730 $\pm$ 3 Torr	$\text{CH}_2\text{O}, \text{HC(O)OH}$	Neeb et al., <sup>25</sup> 1998
0.40–0.50	295 $\pm$ 2 K and 730 $\pm$ 3 Torr	$\text{HC(O)OH}$ , $\text{CH}_3\text{C(O)OH}$ , $\text{CH}_3\text{OH}$	Neeb et al., <sup>24</sup> 1996
$0.39 \pm 0.05$	298 K and 1 atm	$\text{SO}_2$	Hatakeyama et al., <sup>22</sup> 1984
$0.35 \pm 0.05$	298 K and 700 Torr	$\text{CH}_2\text{O}$	Niki et al., <sup>21</sup> 1981
$0.37 \pm 0.02$	282–303 K and 700 Torr	$\text{CH}_2\text{O}$	Kan et al., <sup>20</sup> 1981
0.38	291–299 K and 700 Torr	$\text{CH}_2\text{O}$	Su et al., <sup>19</sup> 1980

In addition, other major products including  $\text{H}_2\text{O} + \text{CO}$  and  $\text{H}_2 + \text{CO}_2$  were also observed in experiments, but these were not included in the analysis by Olzmann et al.<sup>36</sup> In this paper, we focus on the subsequent chemistry of  $\text{CH}_2\text{OO}$  after it has been formed from the ozone plus ethylene reaction. The initial stages of this reaction are well-studied, and the reader is referred to refs 31–37 for background.

In this work, we use high-accuracy extrapolated ab initio thermochemistry (HEAT-345(Q) protocol)<sup>38–40</sup> in combination with a modern and accurate kinetic technique (i.e., semiclassical transition-state theory (SCTST)<sup>41–45</sup> incorporated in a two-dimensional (2D)-master equation model<sup>46</sup>) to reinvestigate the  $\text{O}_3 + \text{C}_2\text{H}_4$  reaction under tropospheric conditions. This reaction, which is a staple in organic chemistry textbooks, holds many puzzles, and some of these are investigated in this work.

## METHODOLOGY

**Quantum Chemical Calculations.** Energies of various species that result from unimolecular dissociation reactions starting with vibrationally excited  $\text{CH}_2\text{OO}$  were calculated using HEAT-345(Q),<sup>38–40</sup> which has been described in detail in previous papers.<sup>38–40</sup> In this work, we have slightly modified two terms in the original HEAT protocol as detailed below:

(i) Zero-point vibrational energies (ZPE) were calculated using the CCSD(T) method (in the frozen-core approximation) in combination with the “NASA Ames” atomic natural orbital (ANO) basis set of Taylor and Almlöf.<sup>47,48</sup> Harmonic force fields were calculated using the ANO2 basis set,<sup>49</sup> while the ANO1 basis set<sup>49</sup> was used to obtain anharmonic force fields. Second-order vibrational perturbation theory (VPT2)<sup>50</sup> was then used to compute anharmonic constants and the corresponding (anharmonic VPT2) ZPE.

(ii) Experimental spin–orbit (SO) corrections are used wherever they are available; experimental SO corrections for hydroxyl radical and triplet oxygen atom are 69.6 and 78  $\text{cm}^{-1}$ ,<sup>51</sup> respectively. However, the other molecules studied in this work are not in degenerate electronic states, so none of them exhibits a first-order SO effect.

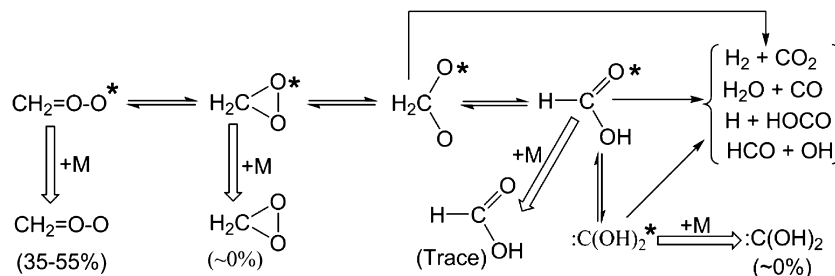
As usual, in coupled-cluster calculations the restricted HF-reference wave function is used for closed-shell molecules, whereas the unrestricted HF-reference wave function is used for open-shell molecules including singlet biradical species (such as methylene bis-oxy,  $\cdot\text{OCH}_2\text{O}\cdot$ ). The CFOUR quantum chemistry program<sup>52</sup> was used for CCSD(T) and CCSDT calculations, while CCSDT(Q) calculations used the MRCC code,<sup>53</sup> as interfaced with the CFOUR.

**Thermochemistry.** It is well-established that the HEAT protocol can provide thermochemical parameters (such as heats of formation, bond dissociation energy, and others) within 1 kJ/mol as compared to experiments for relatively small molecules.<sup>38–40</sup> This appears to remain valid for many of the systems covered in this work; see Table 2 for comparisons of energetics with those from the Active Thermochemical Tables (ATcT). As can be seen, heats of formation calculated with HEAT for formaldehyde, two formic acids and dioxirane are in excellent agreement (within 0.5 kJ/mol) with those of the highly accurate benchmark (ATcT).<sup>54–56</sup> However, for Criegee ( $\text{CH}_2\text{OO}$ ), the HEAT values (109.42 kJ/mol at 0 K and 102.46 kJ/mol at 298 K) are about 4 kJ/mol lower than the those of the ATcT, although the former agree well with other theoretical results (109.9 kJ/mol at 0 K and 102.8 kJ/mol at 298 K) calculated using a similar high accuracy (W3-F12) method<sup>57</sup> (see Table 2). This difference may be due to the fact that there is little other high-quality theoretical work nor much in the way of experiments that are needed to calibrate the ATcT; or, alternatively, it might reflect the fact that  $\text{CH}_2\text{OO}$  has a challenging electronic structure.<sup>58</sup> On the basis of this comparison, however, it is expected that HEAT may also provide

**Table 2. Calculated Heats of Formation (in Kilojoules per Mole) for Various  $\text{CH}_2\text{O}_2$  Species Using HEAT-345(Q) Protocol**

species	$\Delta H_f$ at 0 K	$H(298.15 \text{ K}) - H(0 \text{ K})$	$\Delta H_f$ at 298 K	ATcT (0 K) <sup>a</sup>	ATcT (298 K) <sup>a</sup>
C	711.384	1.050	716.869		
H	216.034	4.234	217.998		
O	246.844	4.340	249.229		
$\text{CH}_2\text{O}$	−105.76	10.020	−109.60	−105.33 $\pm$ 0.11	−109.16 $\pm$ 0.11
<i>trans</i> - $\text{HC(=O)OH}$	−371.76	10.878	−379.08	−371.62 $\pm$ 0.27	−378.94 $\pm$ 0.27
<i>cis</i> - $\text{HC(=O)OH}$	−354.84	11.101	−361.94	−355.28 $\pm$ 0.43	−362.52 $\pm$ 0.43
dioxirane	8.97	10.545	1.32	9 $\pm$ 1.2	1.3 $\pm$ 1.2
$\text{H}_2\text{C=O-O}$ , Criegee	109.42	11.235	102.46	113.4 $\pm$ 1.2 (109.9) <sup>b</sup>	106.3 $\pm$ 1.2 (102.8) <sup>b</sup>
<i>trans-trans</i> - $\text{C(OH)}_2$	−199.12	11.117	−206.20		
<i>cis-trans</i> - $\text{C(OH)}_2$	−196.27	11.114	−203.35		
<i>cis-cis</i> - $\text{C(OH)}_2$	−167.18	11.251	−174.13		
bis-oxy, $^{\circ}\text{O-CH}_2\text{-O}^{\circ}$	54.96	11.430	48.19		

<sup>a</sup>Taken from ATcT, version 1.112.<sup>54–56</sup> <sup>b</sup>Calculated using the W3-F12 level of theory by Karton et al.<sup>57</sup>

Scheme 1. Schematic Reaction Mechanism of Vibrationally Excited Criegee  $\text{CH}_2\text{OO}$  Intermediate<sup>a</sup>

<sup>a</sup>Species designated with an asterisk are present only in highly excited vibrational states.

high accuracy for heats of formation of three different conformers of dihydroxy-carbene as well as methylene bis-oxy. To the best of our knowledge, the present work documents the highest level of theory yet applied to the  $[\text{CH}_2\text{O}_2]$  system.

**Reaction Mechanism.** The chemical reactivity of vibrationally excited Criegee intermediates, which are produced from ozonolysis of olefins (particularly ethylene), has been studied extensively and is well-documented.<sup>3–9</sup> Therefore, only a brief description summarized in Scheme 1 (also see Figure 1A,B) is given here.

As can be seen, about  $45 \pm 10\%$  of hot Criegee  $\text{CH}_2\text{OO}$  is collisionally stabilized by a third body; the remaining hot Criegee rapidly ring closes to dioxirane via TS1 (see Figure 1A) over a barrier of 19.1 kcal/mol. Hot Criegee could also form  $\text{HO} + \text{HCO}$  via 1,3 H-shift, but this step must overcome a very high barrier of 31.8 kcal/mol and thus cannot compete with the ring closure. Dioxirane when formed has a high internal energy (at least 43 kcal/mol), so it ring-opens rapidly via TS3 leading to methylene bis-oxy ( $\cdot\text{OCH}_2\text{O}\cdot$ ), facing a barrier of 26.7 kcal/mol. The dioxirane ( $\text{CH}_2\text{O}_2$ ) intermediate was observed at 77 K in the gas-phase,<sup>59,60</sup> but has not yet been detected in the solution phase,<sup>61</sup> so its degree of stabilization could be very small. Methylene bis-oxy ( $\cdot\text{OCH}_2\text{O}\cdot$ ) can then proceed either 1,2 H-migration via TS4 to formic acid or  $\text{H}_2$ -elimination via TS5 to  $\text{H}_2 + \text{CO}_2$ . These two pathways have very low barriers (1–2 kcal/mol); thus, methylene bis-oxy is a very unstable intermediate, as might be expected for a singlet biradical species. Once formed, formic acid has a very high internal energy of about 115 kcal/mol, so it easily dissociates to  $\text{H}_2\text{O} + \text{CO}$  or  $\text{H}_2 + \text{CO}_2$  via low-lying transition states (TS6 or TS7). Collisional stabilization of vibrationally excited intermediate formic acid under atmospheric conditions is highly unlikely. A small fraction (<5%) of formic acid was experimentally detected,<sup>3</sup> but this more likely arises from reactions of cold  $\text{CH}_2\text{OO}$  with  $\text{H}_2\text{O}$  and/or  $\text{CH}_2\text{O}$  rather than being due to collisional stabilization of hot formic acid. Vibrationally excited formic acid could also dissociate to numerous radical products such as  $\text{H} + \text{HOCO}$  or  $\text{HO} + \text{HCO}$ , but these paths are only minor although energetically accessible. Finally, hot formic acid can isomerize (by 1,2 H-shift via TS8 or TS9) to dihydroxy-carbene, followed by rapid decomposition of dihydroxy-carbene to various products. Recently, three conformers of dihydroxy-carbene have been determined experimentally,<sup>62,63</sup> but they will not be formed from the title reaction.

A comparison of the current work with the previous results for decomposition of hot  $\text{CH}_2\text{OO}$  is given in Table S3 in the Supporting Information. Inspection of Table S3 shows that the HEAT values are in difference of 1–5 kcal/mol with lower-level

theoretical calculations.<sup>31,62,64</sup> Such difference is neither surprising nor a cause for concern.

In summary, the hot Criegee  $\text{CH}_2\text{OO}$  intermediate produced from reaction of  $\text{O}_3$  with  $\text{C}_2\text{H}_4$  is stabilized partly by collisions with a third body; the remaining  $\text{CH}_2\text{OO}$  molecules with an excess of internal energy will rapidly convert to formic acid, followed by decomposition of hot formic acid leading to several products. The reaction mechanism characterized in this work (as displayed in Figure 1A,B and Scheme 1) is in accordance with both conventional wisdom and the numerous products that have been detected experimentally.<sup>1–30</sup>

**Chemical Kinetics Analysis.** As should be clear from the preceding section, the chemical reaction mechanism of hot Criegee intermediate is very complicated; it takes place through multiple intermediates and yields multiple products. In addition, it also includes a delicate competition between unimolecular reactions (i.e., dissociation–isomerization) of intermediates and collisional energy-transfer processes of intermediates with a third body. A master equation technique is needed to determine yields of different products and collisionally stabilized intermediates as functions of both temperature and pressure.

To solve a master equation for the system under study, one needs to know the nascent energy distribution function of hot Criegee just produced from ozonolysis of ethylene. Therefore, one first needs to solve a master equation that governs the reaction of  $\text{O}_3$  with  $\text{C}_2\text{H}_4$ . The potential energy surface of the reaction between  $\text{O}_3$  and  $\text{C}_2\text{H}_4$  leading to hot Criegee  $\text{CH}_2\text{OO}$  (see Figure 2) has been computed by Wheeler et al.<sup>65</sup> using the high-accuracy focal point method and is adopted here for chemical kinetics analysis. Note that in Figure 2 only the concerted dissociation of energized POZ leading to  $\text{CH}_2\text{OO} + \text{H}_2\text{O}$  is considered. The decomposition of energized POZ via an additional stepwise mechanism giving both  $\text{CH}_2\text{OO} + \text{H}_2\text{O}$  and  $\text{HO}$  radical (see Figure S4 in the Supporting Information) will be mentioned in the next section. Here, the van der Waals complex of  $\text{O}_3$  with  $\text{C}_2\text{H}_4$  (see Figure 2) is assumed to be in microcanonical equilibrium with the initial reactants, so it does not play a role in kinetics and can be ignored. A two-dimensional ( $E, J$ )-grained master-equation that depends explicitly on both total internal energy ( $E$ ) and total angular momentum number ( $J$ ) and describes the competition between unimolecular reactions and the collisional energy process between the primary ozonide (POZ) and a third body is given in eq 1:

$$\frac{d[C(E_i, J_i)]}{dt} = R \cdot F(E_i, J_i) - (k_1(E_i, J_i) + k_2(E_i, J_i))[C(E_i, J_i)] - \omega[C(E_i, J_i)] + \omega \sum_{J_k=0}^{\infty} \sum_{E_k=0}^{\infty} P(E_i, J_i | E_k, J_k) [C(E_k, J_k)] \quad (1)$$

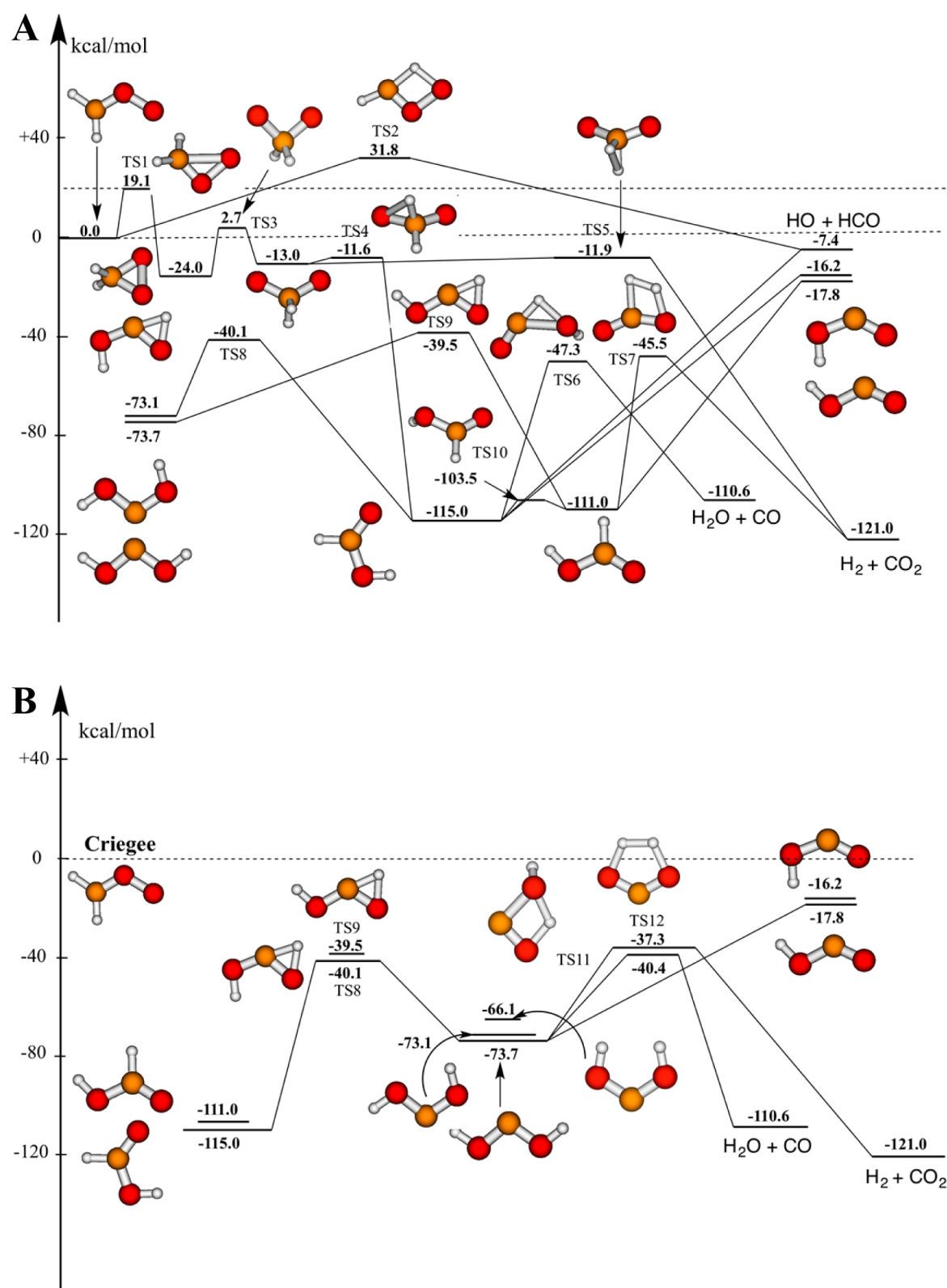


**Figure 1.** Schematic reaction energy profile for decomposition of hot Criegee  $\text{CH}_2\text{OO}$  intermediate constructed using the HEAT-345(Q) level of theory.

where  $C$  is the population of the vibrationally excited POZ intermediate;  $\omega$  is the collision frequency of the POZ with a third body;  $k_1$  and  $k_2$  are the microcanonical rate constants for the  $\text{POZ} \rightarrow \text{O}_3 + \text{C}_2\text{H}_4$  step and the  $\text{POZ} \rightarrow \text{CH}_2\text{OO} + \text{CH}_2\text{O}$  step, respectively.  $P(E_i, J_i | E_k, J_k)$  represents the probability

function for energy and angular momentum transfer from state  $(E_k, J_k)$  to state  $(E_i, J_i)$ .  $R \cdot F$  is the source term where  $R$  is the total rate of the entrance flux for formation of POZ (e.g., the  $\text{O}_3 + \text{C}_2\text{H}_4 \rightarrow \text{POZ}$  step;  $R$  is set to be unity to compute product branching ratios) and  $F$  is the initial energy–angular



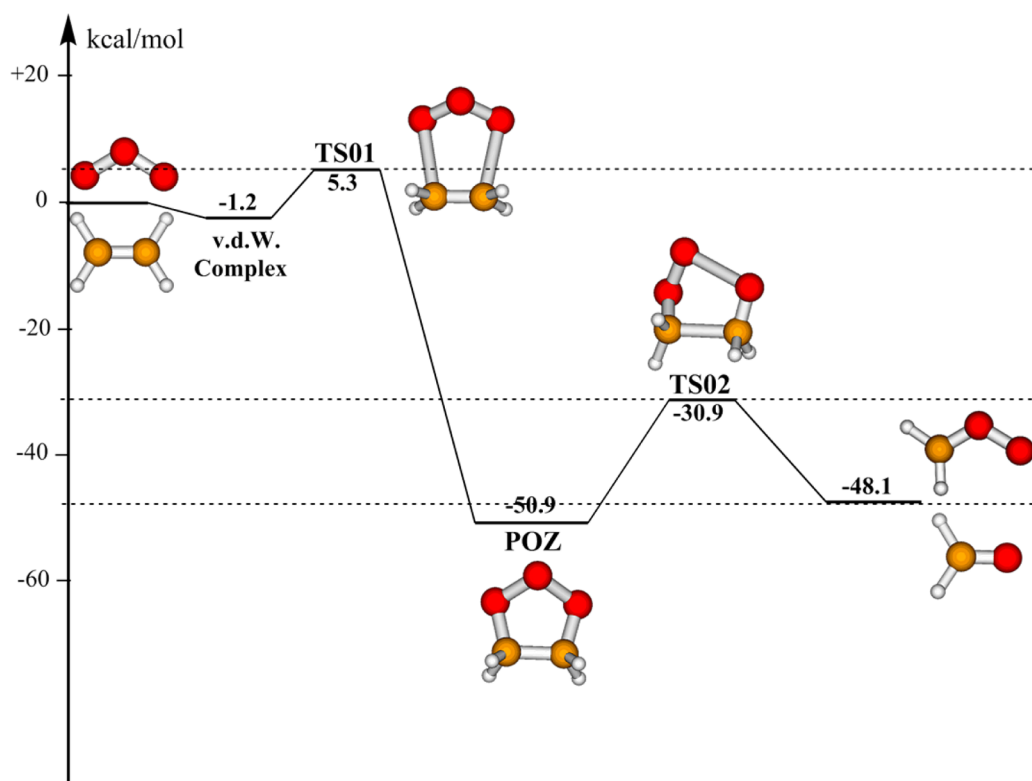


**Figure 2.** Schematic reaction energy profile of the formation of hot Criegee  $\text{CH}_2\text{OO}$  intermediate from the  $\text{O}_3 + \text{C}_2\text{H}_4$  reaction, adopted from the work of Wheeler et al.<sup>65</sup> who used the focal point method.

momentum distribution function of POZ, which is given by eq 2:<sup>66–68</sup>

$$F(E, J) = \frac{(2J + 1)G(E, J) \exp\left(-\frac{E}{kT}\right)}{\sum_{J=0}^{\infty} \int_0^{\infty} (2J + 1)G(E, J) \exp\left(-\frac{E}{kT}\right) dE} \quad (2)$$

A graphical representation of  $F(E, J)$  at  $T = 300$  K is displayed in Figure 3. An expectation value of 40 for the total angular momentum ( $\langle J \rangle$ ) can then be computed using eq 3.

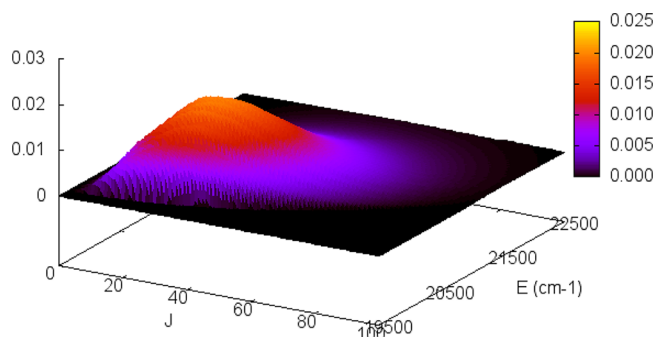


**Figure 3.** Initial energy and angular momentum distribution function ( $F(E, J) \times 100$ ), depending on both internal energy, constructed with  $\Delta E = 10 \text{ cm}^{-1}$  and angular momentum  $\Delta J = 1$  of primary ozonide (POZ) at 300 K, which is just formed from the addition of  $\text{O}_3$  onto  $\text{C}_2\text{H}_4$ .

$$\langle J \rangle = \frac{\sum_{J=0}^{\infty} J \cdot \int_0^{\infty} F(E, J) dE}{\sum_{J=0}^{\infty} \int_0^{\infty} F(E, J) dE} \quad (3)$$

Note that eq 1 is intended for a single-well master equation. The extension to a multiple-intermediate master equation is straightforward and can be found in our recent 2DME paper (ref 46) and also in the literature (refs 69 and 70). For the reaction starting with nascent Criegee (see Scheme 1 and Figure 1), there are five different intermediates:  $\text{CH}_2\text{OO}$  (1), dioxirane (2), methylene bisoxo (3), formic acid (4), and dihydroxy-carbene (5); thus, eq 1 can be rewritten as eqs 1a to 1e to take these five intermediates into account:

$$\begin{aligned} \frac{d[C_1(E_i, J_i)]}{dt} &= F(E_i, J_i) - \left( \sum k_1(E_i, J_i) + k_{2 \leftarrow 1}(E_i, J_i) \right) [C_1(E_i, J_i)] \\ &\quad - \omega [C_1(E_i, J_i)] + \omega \sum_{J_k=0}^{\infty} \sum_{E_k=0}^{\infty} P(E_i, J_i | E_k, J_k) [C_1(E_k, J_k)] \\ &\quad + k_{1 \leftarrow 2}(E_i, J_i) [C_2(E_i, J_i)] \end{aligned} \quad (1a)$$

$$\begin{aligned} \frac{d[C_2(E_i, J_i)]}{dt} &= - \left( \sum k_2(E_i, J_i) + k_{1 \leftarrow 2}(E_i, J_i) + k_{3 \leftarrow 2}(E_i, J_i) \right) [C_2(E_i, J_i)] \\ &\quad - \omega [C_2(E_i, J_i)] + \omega \sum_{J_k=0}^{\infty} \sum_{E_k=0}^{\infty} P(E_i, J_i | E_k, J_k) [C_2(E_k, J_k)] \\ &\quad + k_{2 \leftarrow 1}(E_i, J_i) [C_1(E_i, J_i)] + k_{2 \leftarrow 3}(E_i, J_i) [C_3(E_i, J_i)] \end{aligned} \quad (1b)$$

$$\begin{aligned} \frac{d[C_3(E_i, J_i)]}{dt} &= - \left( \sum k_3(E_i, J_i) + k_{2 \leftarrow 3}(E_i, J_i) \right. \\ &\quad \left. + k_{4 \leftarrow 3}(E_i, J_i) \right) [C_3(E_i, J_i)] - \omega [C_3(E_i, J_i)] \\ &\quad + \omega \sum_{J_k=0}^{\infty} \sum_{E_k=0}^{\infty} P(E_i, J_i | E_k, J_k) [C_3(E_k, J_k)] \\ &\quad + k_{3 \leftarrow 2}(E_i, J_i) [C_2(E_i, J_i)] + k_{3 \leftarrow 4}(E_i, J_i) [C_4(E_i, J_i)] \end{aligned} \quad (1c)$$

$$\begin{aligned} \frac{d[C_4(E_i, J_i)]}{dt} = & -(\sum k_4(E_i, J_i) + k_{3 \leftarrow 4}(E_i, J_i)) \\ & + k_{5 \leftarrow 4}(E_i, J_i)[C_4(E_i, J_i)] - \omega[C_4(E_i, J_i)] \\ & + \omega \sum_{J_k=0}^{\infty} \sum_{E_k=0}^{\infty} P(E_i, J_i | E_k, J_k) [C_4(E_k, J_k)] \\ & + k_{4 \leftarrow 3}(E_i, J_i)[C_3(E_i, J_i)] + k_{4 \leftarrow 5}(E_i, J_i)[C_5(E_i, J_i)] \end{aligned} \quad (1d)$$

$$\begin{aligned} \frac{d[C_5(E_i, J_i)]}{dt} = & -(\sum k_5(E_i, J_i) + k_{4 \leftarrow 5}(E_i, J_i)) [C_5(E_i, J_i)] \\ & - \omega[C_5(E_i, J_i)] + \omega \sum_{J_k=0}^{\infty} \sum_{E_k=0}^{\infty} P(E_i, J_i | E_k, J_k) [C_5(E_k, J_k)] \\ & + k_{5 \leftarrow 4}(E_i, J_i)[C_4(E_i, J_i)] \end{aligned} \quad (1e)$$

where  $k_{j \leftarrow i}(E, J_i)$  and  $k_{i \leftarrow j}(E, J_i)$  are the microcanonical rate coefficients for isomerization step from well  $i$  to well  $j$  and vice versa.

The two-dimensional  $(E, J)$ -grained master equation (eq 1), assuming the steady-state condition, is solved (see eq 4 for thermal rate constants  $k(T, P)$  and eq 5 for yields  $\gamma(T, P)$ ) using a program (named 2DME-SSS)<sup>46</sup> soon to be included in the MULTIWELL suite.<sup>71</sup>

$$\langle k(T, P) \rangle = \frac{\sum_{J=0}^{\infty} k(T, P)_J \cdot \int_0^{\infty} F(E, J) dE}{\sum_{J=0}^{\infty} \int_0^{\infty} F(E, J) dE} \quad (4)$$

$$\langle \gamma(T, P) \rangle = \frac{\sum_{J=0}^{\infty} \gamma(T, P)_J \cdot \int_0^{\infty} F(E, J) dE}{\sum_{J=0}^{\infty} \int_0^{\infty} F(E, J) dE} \quad (5)$$

For the  $O_3 + C_2H_4$  reaction and the subsequent chemistry of hot  $CH_2OO$  related to the tropospheric chemistry, parameters used in the 2DME are obtained as follows: the ceiling energy is chosen to be  $70\,000\text{ cm}^{-1}$  with a grain size of  $10\text{ cm}^{-1}$ ; the maximum angular momentum value of  $J$  is 200 and the step size  $\Delta J$  is 5. Air (an 80:20 mixture of  $N_2/O_2$ ) is chosen to be the bath gas, whose collisional parameters<sup>72</sup> are given in Table S1 in the Supporting Information. For intermediates and well-defined TSs, densities and sums of states are counted exactly with a bin size of  $10\text{ cm}^{-1}$  using ADENSUM<sup>73</sup> and SCTST<sup>44,45</sup> codes, respectively. The two rotamers of formic acid are considered as a composite species by treating the hindered internal rotor of the H atom around the C–O axis. The same approach is applied to three conformers of dihydroxy-carbene. For reaction paths without exit TSs (e.g.,  $HC(O)OH \rightarrow HCO + OH$ ), the microcanonical variational Rice–Ramsperger–Kassel–Marcus (RRKM) theory<sup>74,75</sup> is used to locate a kinetic bottleneck geometry. First, geometries of points (considering a bond length from 2.0 to 3.0 Å with a step size of 0.1 Å) along the reaction coordinate are otherwise optimized (i.e., the bond length along the reaction coordinate is fixed, whereas the remaining coordinates are allowed to relax freely) using the FC-CCSD(T)/ANO1 level of theory based on the unrestricted HF-reference wave function. Then, a harmonic oscillator analysis is done with the same method to obtain rovibrational parameters. Finally, these rovibrational parameters and relative energies of all grid points are input to the 2DME-SSS code, which uses a cubic spline interpolation technique<sup>76</sup> to obtain the required parameters for

intermediate points. 2DME-SS then computes sum of states as functions of both energy and angular momentum for each grid point to find a kinetic bottleneck structure over a grid of geometries (as characterized by the bond length that runs from 2 to 3 Å) with a resolution (step size) of 0.01 Å.

Our calculations show that the fraction of collisional stabilized POZ is negligible under all conditions in the atmosphere; the fraction of  $CH_2O$  formation is unity. These conclusions are insensitive to the level of theory and furthermore consistent with previous experimental<sup>15–30</sup> and theoretical findings.<sup>36</sup> The master equation calculations also provide the steady-state population of POZ, which is then used to construct the initial energy–angular momentum distribution function for hot nascent  $CH_2OO$  using the separate statistical ensembles (SSE) method.<sup>74</sup> The SSE technique, which is well-documented<sup>77–83</sup> (also see a summary of SSE method given in Table S2 in the Supporting Information), is found to work fairly well for similar reaction systems<sup>78–83</sup> (including hot CIs produced from ozonolysis of  $\beta$ -pinene<sup>83</sup>) where secondary chemistry of the separating fragments is important. As an example, the nascent population of  $CH_2OO$  calculated at an expectation value of  $\langle J \rangle = 40$  as a function of energy is presented in Figure 4 at the

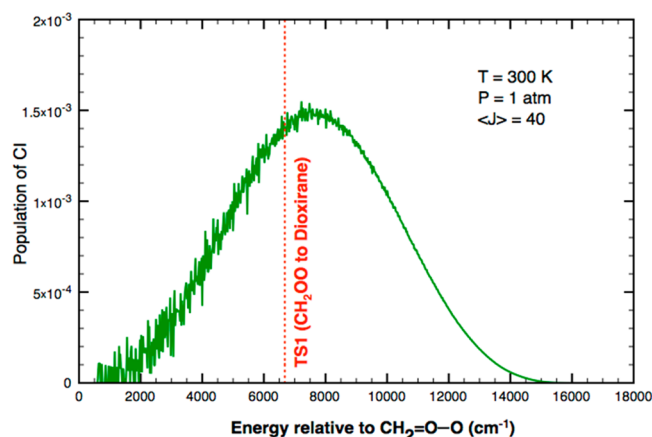


**Figure 4.** Nascent energy distribution function of vibrationally excited Criegee  $CH_2=O-O$  intermediate, which is just formed from the  $O_3 + C_2H_4$  reaction at the conditions of 300 K and 1 atm and an expectation angular momentum of 40.

conditions of 300 K and 1 atm. The initial energy–angular momentum distribution of nascent  $CH_2OO$  is then used as input for the 2DME-SSS code to compute product branching ratios. In the 2DME model (ref 46), we have assumed that total angular momentum does not change by collisions between energized intermediates and bath gases (i.e., fixed- $J$  model); therefore, total angular momentum is always conserved from the initial reactants ( $C_2H_4 + O_3$ ) through intermediate POZ via transition states (TS01 and TS02) to products ( $CH_2OO + H_2O$ ). In other words, the nascent energy distribution of Criegee is calculated at a fixed angular momentum.

At  $T = 300\text{ K}$  and  $P = 1\text{ atm}$ , the prediction for the yield of stabilized  $CH_2OO$  is about  $0.48 \pm 0.05$ , which is in excellent agreement with all available experimental data (see Table 1), but about twice as large as the theoretical results ( $\gamma_{SCI} = 0.21$  to 0.29) reported by Olzmann et al.,<sup>36</sup> who used the one-dimensional master equation technique. Interestingly, we also obtain a similar result of 0.27 for the SCI fraction when angular momentum effects are excluded (i.e.,  $J = 0$ ). Therefore, it would seem that

angular momentum effects play an important role for bringing theoretical results into line with the experiments (see Table 1). A plausible error bar of 0.05 (e.g., 5%) is obtained by carrying out a simple sensitivity analysis (i.e., by shifting the barrier height of TS1, which is the rate-determining transition structure for the ring-closure step from CH<sub>2</sub>OO to dioxirane (see Figure 1A), up and down by 0.25 kcal/mol, the usual error bar with HEAT protocol and varying the value for downward energy transfer from 100 to 500 cm<sup>-1</sup>,<sup>72</sup> which covers all plausible values for collisions of the [CH<sub>2</sub>O<sub>2</sub>] system with air (N<sub>2</sub>/O<sub>2</sub> ≈ 80/20) (see Figure S2 in the Supporting Information)).

Furthermore, the pressure effects are also investigated. The yield of the stabilized CH<sub>2</sub>OO increases moderately when pressure rises; it starts with  $\gamma_{\text{SCI}} = 0.36$  at 1 Torr and reaches  $\gamma_{\text{SCI}} = 0.48$  at 1000 Torr (see Figure S3 in the Supporting Information). Even at lower pressures, the SCI fraction does not become zero. Figure 4 is instructive in this regard. The part (which comprises a fraction of 0.34) below TS1 (for the CH<sub>2</sub>OO → dioxirane step) in Figure 4 is chemically inactive and is collisionally stabilized even at low pressures. These findings are moreover consistent with the experimental results of Hatakeyama et al.<sup>21,22</sup>

The SCI yield is found to be weakly dependent on temperature (see Figure 5). The yield of SCI calculated with the 1DME

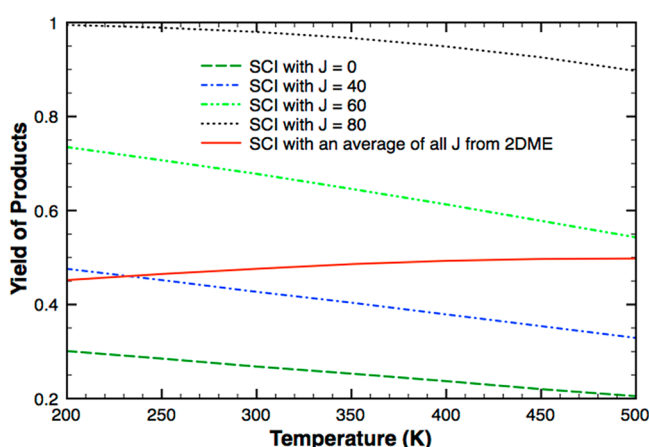


**Figure 5.** Fraction of the collisional stabilized Criegee CH<sub>2</sub>OO intermediate calculated at 1 atm as a function of temperature.

method at each discrete angular momentum value decreases when temperature increases in the range of 200–500 K, whereas the rotationally averaged yield of SCI increases marginally from ca. 0.45 to 0.50 when the 2DME method is used.

In addition to the stabilized CH<sub>2</sub>OO product, the 2DME calculations also provide yields for other products including H<sub>2</sub>O + CO ( $\gamma = 0.31$ ), H<sub>2</sub> + CO<sub>2</sub> (0.18), H + HOCO (0.02), and HO + HCO (0.02) from subsequent dissociation of hot CH<sub>2</sub>OO

at 300 K and 1 atm. The calculations also show that the stabilized fractions for formic acid, dioxirane, and dihydroxy-carbene are negligible under all tropospheric conditions. The product yields of H<sub>2</sub>O + CO and H<sub>2</sub> + CO<sub>2</sub> are in good agreement with the experiments (see Table 3), whereas the HO radical product (ca. 2%) is significantly underestimated (experiments find 8–17%).<sup>3,15–30,35</sup> The low predicted yield of OH is entirely expected, however, because the HO radical product path from CH<sub>2</sub>OO cannot compete with the other reaction paths (see Figure 1A). This suggests that much of the HO radical product seen experimentally could be produced from a mechanism other than the dissociation of hot Criegee. O’Neal and Blumstein<sup>34</sup> proposed a new mechanism for the gas-phase ozone–olefin reactions, in which biradical intermediates, formed in the stepwise decomposition mechanism of POZ, could react by an  $\alpha$ -H-abstraction path leading to  $\alpha$ -keto hydroperoxide, which was believed to be detected experimentally in the *cis*-2-butene + O<sub>3</sub> reaction.<sup>84</sup> The O’Neal–Blumstein (stepwise) mechanism of dissociation of POZ was theoretically characterized and discussed by Anglada et al. (ref 31). Both stepwise and concerted mechanisms are also summarized in Figure S4 (see the Supporting Information) that was constructed using the CI-PT2(8,8)/aug-cc-pVTZ level of theory.<sup>85</sup> Note that HEAT-345(Q) method is too costly to be applied to the [C<sub>2</sub>H<sub>4</sub>O<sub>3</sub>] system. The CI-PT2 method is a good choice in this case because it compensates between moderate accuracy and applicability. As seen in Figure S4 in the Supporting Information, in addition to the concerted decomposition mechanism, vibrationally excited POZ can isomerize via a biradical intermediate ( $\cdot\text{OOCH}_2\text{CH}_2\text{O}\cdot$ ) to hydroperoxy methylformate (HOOCH<sub>2</sub>CHO). HOOCH<sub>2</sub>CHO, just formed, with an internal energy of (at least) 103 kcal/mol will immediately decompose to HO + HCO + CH<sub>2</sub>O. Consequently, HO radical product can be formed from this additional stepwise mechanism. Based on the reaction mechanism in Figure S4 in the Supporting Information, our 2DME calculations then give a yield of 11 ± 6% for HO and HCO radicals that are produced through the singlet biradical intermediate  $\cdot\text{OOCH}_2\text{CH}_2\text{O}\cdot$ . Combining these results via the stepwise decomposition mechanism of POZ with those obtained above via the direct mechanism, we have finally obtained product branching ratios for various channels in the O<sub>3</sub> + C<sub>2</sub>H<sub>4</sub> reaction. The results are presented in Table 3, which also includes available experimental data for a direct comparison. Table 3 shows that our results are entirely consistent with all measured values, within the experimental error bars.<sup>15–30</sup>

**Why Has the Stabilized Criegee CH<sub>2</sub>OO Not Yet Been Observed Directly?** Our calculations give 42 ± 6% for the SCI yield (see Table 3), which is in accord with an average value of ca. 45 ± 10% estimated from the experimental results in Table 1. The thermal rate constant for the loss of SCI at room temperature is evaluated to be about 0.3 s<sup>-1</sup> using SCTST. Hence, the lifetime of SCI is estimated to be a couple of seconds, which

**Table 3.** Calculated Yields of Various Products from the O<sub>3</sub> + C<sub>2</sub>H<sub>4</sub> Reaction at  $T = 300$  K and  $P = 1$  atm<sup>a</sup>

products	this work	Su et al. <sup>b</sup>	Horie et al. <sup>c</sup>	Neeb et al. <sup>d</sup>	Copeland et al. <sup>e</sup>	Alam et al. <sup>f</sup>
SCI	0.42 ± 0.06	0.38 ± 0.06	0.47	0.50	N/A	0.54 ± 0.12
H <sub>2</sub> O + CO	0.27 ± 0.06	0.36 ± 0.06	0.31	0.23	0.25 ± 0.02	0.24
HO + HCO	0.13 ± 0.06		N/A		N/A	0.17 ± 0.09
H <sub>2</sub> + CO <sub>2</sub>	0.16 ± 0.06		0.13	0.23	0.18 ± 0.02	
H + HOCO	0.02	0.22 ± 0.04	0.09			0.05
HC(O)OH	0.00	0.04 ± 0.01	0.00	0.04	0.04 ± 0.01	0.00
CH <sub>2</sub> O	1.00	≈1.00	≈1.00	≈1.00	≈0.89 ± 0.09	1.00

<sup>a</sup>Available experimental data are also included for the purpose of comparison. <sup>b</sup>Ref 16. <sup>c</sup>Ref 29. <sup>d</sup>Ref 25. <sup>e</sup>Ref 30. <sup>f</sup>Ref 28.

in principle should be long enough for spectroscopic detection. Nonetheless, the stabilized Criegee produced from the  $\text{O}_3 + \text{C}_2\text{H}_4$  reaction has not yet been observed directly. Recently, “cool” Criegees ( $\text{CH}_2\text{OO}$ ,  $\text{CH}_3\text{CHOO}$ ,  $(\text{CH}_3)_2\text{COO}$ , and  $\text{C}_2\text{H}_5\text{CHOO}$ ), which are produced from other kinds of reactions and different techniques, have been detected spectroscopically.<sup>11–18</sup> These findings raise a question: why has the stabilized  $\text{CH}_2\text{OO}$  from the  $\text{O}_3 + \text{C}_2\text{H}_4$  not yet been detected? We suggest two possible reasons: (1) It rapidly reacts with the initial reactants (i.e.,  $\text{C}_2\text{H}_4$ , or  $\text{O}_3$  which are present in great excess) or any possible contaminants, e.g.  $\text{H}_2\text{O}$ ,  $\text{CH}_2\text{O}$ , once formed. (2) Once stabilized, it rapidly reacts with other products from the “hot” channel, i.e.  $\text{H}_2\text{O}$ ,  $\text{CH}_2\text{O}$ , etc. Because the branching ratio between “cold” and “hot” is roughly 50/50, stoichiometrically there is enough product from the “hot” channel to react with all of the “cold”  $\text{CH}_2\text{OO}$ . As a result, the SCI vanishes before it can be detected. Note that these subsequent reactions have not been investigated here. The recent experimental studies<sup>86–88</sup> have shown the very fast reaction of  $\text{CH}_2\text{OO}$  with water dimer, with a rate of about  $(4–6) \times 10^{-12} \text{ cm}^3 \text{ molecule}^{-1} \text{ s}^{-1}$ ,<sup>86–88</sup> which is in close agreement with an early theoretical prediction.<sup>89</sup> This result seems to indicate that the reaction of  $\text{CH}_2\text{OO}$  with water (that is one of main products) is a major sink that could cause a fast disappearance of thermalized Criegee in experiments.

There is another plausible explanation, which assumes a fast dissociation of the stabilized  $\text{CH}_2\text{OO}$  to  $\text{CH}_2\text{O} + \text{O}(^3\text{P})$ . If this happened, the  $\text{CH}_2\text{O}$  yield would be greater than unity (e.g.,  $\text{C}_2\text{H}_4 + \text{O}_3 \rightarrow \text{CH}_2\text{O} + \text{CH}_2\text{OO} \rightarrow 2\text{CH}_2\text{O} + \text{O}(^3\text{P})$ ). This, however, is contrary to the experimental evidence that always shows a yield of unity for  $\text{CH}_2\text{O}$ . In addition, there is no experimental evidence for  $\text{O}(^3\text{P})$  formation in the  $\text{O}_3 + \text{C}_2\text{H}_4$  reaction. The yield of triplet oxygen atom formation from ozonolysis of olefin is estimated to be smaller than 4%.<sup>3</sup> Furthermore, the  $\text{CH}_2\text{OO} \rightarrow \text{CH}_2\text{O} + \text{O}(^3\text{P})$  reaction is a spin-forbidden process. To produce  $\text{CH}_2\text{O} + \text{O}(^3\text{P})$ ,  $\text{CH}_2\text{OO}$  must go over a crossing point (or a seam), which lies about 24.8 kcal/mol<sup>90</sup> above  $\text{CH}_2\text{OO}$ . Therefore, in term of energetics, this intersystem-crossing step cannot compete with ring-closure from  $\text{CH}_2\text{OO}$  to dioxirane, which requires only 19 kcal/mol to occur. Therefore, we conclude that fast thermal dissociation of the collisional stabilized  $\text{CH}_2\text{OO}$  to produce  $\text{CH}_2\text{O} + \text{O}(^3\text{P})$  can be dismissed as a possibility.

## CONCLUSIONS

The complex and challenging reaction mechanism and chemical kinetics of vibrationally excited Criegee  $\text{CH}_2\text{OO}^*$  intermediate, formed from the  $\text{O}_3 + \text{C}_2\text{H}_4$  reaction, have been studied using the high-accuracy quantum chemical calculations in conjunction with the 2DME/SCTST technique. The calculated product branching ratios (as summarized in Table 3) are in excellent agreement with available experimental results, and this appears to be the first time that theory has agreed with experiment for this textbook organic reaction. The collisionally stabilized Criegee intermediate is very reactive and is predicted to react rapidly with other species existing in the reaction system (or to dissociate thermally to several products within a couple of seconds). Therefore, stabilized Criegee intermediate produced from the ozonolysis of ethylene (with a lifetime of a few seconds) is expected to vanish as soon as it is formed. As a result, the SCI has not been detected spectroscopically. Finally, evidence is presented that the hydroxyl radical product is mainly formed by the stepwise decomposition of primary ozonide via the singlet

biradical intermediate,  $\cdot\text{OOCH}_2\text{CH}_2\text{O}\cdot$ , and through hydroperoxy methylformate,  $\text{HOOCH}_2\text{CHO}$ .

## ASSOCIATED CONTENT

### Supporting Information

Optimized geometries, rovibrational parameters, anharmonic constants, thermal rate constants, and energies for various species in the reaction of hot  $\text{CH}_2\text{OO}$ . The Supporting Information is available free of charge on the ACS Publications website at DOI: 10.1021/acs.jpca.5b02088.

## AUTHOR INFORMATION

### Corresponding Author

\*E-mail: jfstanton@mail.utexas.edu.

### Notes

The authors declare no competing financial interest.

## ACKNOWLEDGMENTS

J.F.S. and T.L.N. are supported by the Robert A. Welch Foundation (Grant F-1283). This material is based on work supported by the U.S. Department of Energy, Office of Basic Energy Sciences under Award DE-FG02-07ER15884. M.C.M. is supported by National Science Foundation Grant CHE-1058063.

## REFERENCES

- (1) Criegee, R.; Wenner, G. Die Ozonisierung Des 9, 10-Oktalins. *Chem. Ber.* **1949**, *564*, 9–15.
- (2) Criegee, R. Mechanism of Ozonolysis. *Angew. Chem., Int. Ed. Engl.* **1975**, *14*, 745–752.
- (3) Atkinson, R. Gas-Phase Tropospheric Chemistry of Volatile Organic Compounds: 1. Alkanes and Alkenes. *J. Phys. Chem. Ref. Data* **1997**, *26*, 215–290.
- (4) Johnson, D.; Marston, G. The Gas-Phase of Unsaturated Volatile Organic Compounds in the Troposphere. *Chem. Soc. Rev.* **2008**, *37*, 699–716.
- (5) Vereecken, L.; Francisco, J. S. Theoretical Studies of Atmospheric Reaction mechanisms in the Troposphere. *Chem. Soc. Rev.* **2012**, *41*, 6259–6293.
- (6) Alam, M. S.; Rikard, A. R.; Camredon, M.; Wyche, K. P.; Carr, T.; Hornsby, K. E.; Monks, P. S.; Bloss, W. J. Radical Product Yields from the Ozonolysis of Short Chain Alkenes under Atmospheric Boundary Layer Conditions. *J. Phys. Chem. A* **2013**, *117*, 12468–12483.
- (7) Taatjes, C. A.; Shallcross, D. E.; Percival, C. J. Research Frontiers in the Chemistry of Criegee Intermediates and Tropospheric Ozonolysis. *Phys. Chem. Chem. Phys.* **2014**, *16*, 1704–1718.
- (8) Donahue, N. M.; Drozd, G. T.; Epstein, S. A.; Presto, A. A.; Kroll, J. H. Adventures in Ozoneland: Down the Rabbit-Hole. *Phys. Chem. Chem. Phys.* **2011**, *13*, 10848–10857.
- (9) Percival, C. J.; Welz, O.; Eskola, A. J.; Savee, J. D.; Osborn, D. L.; Topping, D. O.; Lowe, D.; Utembe, S. R.; Bacak, A.; McFiggans, G.; Cooke, M. C.; Xiao, P.; Archibald, A. T.; Jenkin, M. E.; Derwent, R. G.; Riipinen, I.; Mok, D. W. K.; Lee, E. P. F.; Dyke, J. M.; Taatjes, C. A.; Shallcross, D. E. Regional and Global Impacts of Criegee Intermediates on Atmospheric Sulphuric Acid Concentrations and First Steps of Aerosol Formation. *Faraday Discuss.* **2013**, *165*, 45–73.
- (10) Vereecken, L. Lifting the Veil on an Old Mystery. *Science (Washington, DC, U.S.)* **2013**, *340*, 154–155.
- (11) Taatjes, C. A.; Meloni, G.; Selby, T. M.; Trevitt, A. J.; Osborn, D. L.; Percival, C. J.; Shallcross, D. E. Direct Observation of the Gas-Phase Criegee Intermediate ( $\text{CH}_2\text{OO}$ ). *J. Am. Chem. Soc.* **2008**, *130*, 11883–11885.
- (12) Welz, O.; Savee, J. D.; Osborn, D. L.; Vasu, S. S.; Percival, C. J.; Shallcross, D. E.; Taatjes, C. A. Direct Kinetic Measurements of Criegee Intermediate ( $\text{CH}_2\text{O}$ ) Formed by Reaction of  $\text{CH}_2\text{I}$  with  $\text{O}_2$ . *Science (Washington, DC, U.S.)* **2012**, *335*, 204–207.



- (13) Su, Y. T.; Huang, Y. H.; Witek, H. A.; Lee, Y. L. Infrared Absorption Spectrum of the Simplest Criegee Intermediate  $\text{CH}_2\text{OO}$ . *Science (Washington, DC, U.S.)* **2013**, *340*, 174–176.
- (14) Taatjes, C. A.; Welz, O.; Eskola, A. J.; Savee, J. D.; Scheer, A. M.; Shallcross, D. E.; Rotavera, B.; Lee, E. P. F.; Dyke, J. M.; Mok, D. K. W.; Osborn, D. L.; Percival, C. J. Direct Measurements of Conformer-Dependent Reactivity of the Criegee Intermediate  $\text{CH}_3\text{CHOO}$ . *Science (Washington, DC, U.S.)* **2013**, *340*, 177–180.
- (15) McCarthy, M. C.; Cheng, L.; Crabtree, K. N.; Martinez, O., Jr.; Nguyen, T. L.; Womack, C. C.; Stanton, J. F. The Simplest Criegee Intermediate ( $\text{H}_2\text{C}=\text{O}-\text{O}$ ): Isotopic Spectroscopy, Equilibrium Structure, and Possible Formation from Atmospheric Lightning. *J. Phys. Chem. Lett.* **2013**, *23*, 4133–4139.
- (16) Beames, J. M.; Liu, F.; Lu, L.; Lester, M. I. Ultraviolet Spectrum and Photochemistry of the Simplest Criegee Intermediate  $\text{CH}_2\text{OO}$ . *J. Am. Chem. Soc.* **2012**, *134*, 20045–20048.
- (17) Beames, J. M.; Liu, F.; Lu, L.; Lester, M. I. UV Spectroscopic Characterization of an Alkyl Substituted Criegee Intermediate  $\text{CH}_3\text{CHOO}$ . *J. Chem. Phys.* **2013**, *138*, 244307 (1–9).
- (18) Liu, F.; Beames, J. M.; Green, A. M.; Lester, M. I. UV Spectroscopic Characterization of Dimethyl- and Ethyl-Substituted Carbonyl Oxides. *J. Phys. Chem. A* **2014**, *118*, 2298–2306.
- (19) Su, F.; Calvert, J. G.; Shaw, J. H. A FT IR Spectroscopic Study of the Ozone-Ethene Reaction Mechanism in  $\text{O}_2$ -Rich Mixtures. *J. Phys. Chem.* **1980**, *84*, 239–246.
- (20) Kan, C. S.; Su, F.; Calvert, J. G.; Shaw, J. H. Mechanism of the Ozone-Ethene Reaction in Dilute  $\text{N}_2/\text{O}_2$  Mixtures Near 1-atm Pressure. *J. Phys. Chem.* **1981**, *85*, 2359–2363.
- (21) Niki, H.; Maker, P. D.; Savage, C. M.; Breitenbach, L. P. A FT IR Study of a Transitory Product in the Gas-Phase Ozone-Ethylene Reaction. *J. Phys. Chem.* **1981**, *85*, 1024–1027.
- (22) Hatakeyama, S.; Kobayashi, H.; Akimoto, H. Gas-Phase Oxidation of  $\text{SO}_2$  in the Ozone-Olefin Reactions. *J. Phys. Chem.* **1984**, *88*, 4736–4739.
- (23) Hatakeyama, S.; Kobayashi, H.; Lin, Z.-Y.; Takagi, H.; Akimoto, H. Mechanism for the Reaction of  $\text{CH}_2\text{OO}$  with  $\text{SO}_2$ . *J. Phys. Chem.* **1986**, *90*, 4131–4135.
- (24) Neeb, P.; Horie, O.; Moortgat, G. K. Gas-Phase Ozonolysis of Ethene in the Presence of Hydroxylic Compounds. *Int. J. Chem. Kinet.* **1996**, *28*, 721–730.
- (25) Neeb, P.; Horie, O.; Moortgat, G. K. The Ethene-Ozone Reaction in the Gas Phase. *J. Phys. Chem. A* **1998**, *102*, 6778–6785.
- (26) Horie, O.; Schafer, C.; Moortgat, G. K. High Reactivity of Hexafluoro Acetone toward Criegee Intermediates in the Gas-Phase Ozonolysis of Simple Alkenes. *Int. J. Chem. Kinet.* **1999**, *31*, 261–269.
- (27) Hasson, A. S.; Orzechowska, G.; Paulson, S. E. Production of Stabilized Criegee Intermediates and Peroxides in the Gas Phase Ozonolysis of Alkenes. *J. Geophys. Res.* **2001**, *106*, 34131–34142.
- (28) Alam, M. S.; Bloss, W. J.; et al. Total Radicals Yields from Tropospheric Ethene Ozonolysis. *Phys. Chem. Chem. Phys.* **2011**, *13*, 11002–11015.
- (29) Horie, O.; Moortgat, G. K. Decomposition Pathways of the Excited Criegee Intermediates in the Ozonolysis of Simple Alkenes. *Atmos. Environ.* **1991**, *25A*, 1881–1896.
- (30) Copeland, G.; Ghosh, M. V.; Shallcross, D. E.; Percival, C. J.; Dyke, J. M. A Study of the Ethene-Ozone Reaction with Photoelectron Spectroscopy: Measurement of Product Branching Ratios and Atmospheric Implications. *Phys. Chem. Chem. Phys.* **2011**, *13*, 14839–14847.
- (31) Anglada, J. M.; Crehuet, R.; Boffil, J. M. The Ozonolysis of Ethene: A Theoretical Study of the Gas-Phase Reaction mechanism. *Chem.—Eur. J.* **1999**, *5*, 1809–1822.
- (32) Chan, W.-T.; Hamilton, I. P. Mechanism for the Ozonolysis of Ethene and Propene: Reliability of Quantum Chemical Predictions. *J. Chem. Phys.* **2003**, *118*, 1688–1701.
- (33) Wadt, W. R.; Goddard, W. A., III. The Electronic Structure of the Criegee Intermediate. Ramifications for the Mechanism of Ozonolysis. *J. Am. Chem. Soc.* **1975**, *97*, 3004–3021.
- (34) O’Neal, H. E.; Blumstein, C. A New mechanism for Gas Phase Ozone-Olefin Reactions. *Int. J. Chem. Kinet.* **1973**, *5*, 397–413.
- (35) Donahue, N. L.; Kroll, J. H.; Anderson, J. G.; Demerjian, K. L. Direct Observation of OH Production from the Ozonolysis of Olefins. *Geophys. Res. Lett.* **1998**, *25*, 59–62.
- (36) Olzmann, M.; Kraka, E.; Cremer, D.; Gutbrod, R.; Andersson, S. Energetics, Kinetics, and Product Distributions of the Reactions of Ozone with Ethene and 2,3-Dimethyl-2-butene. *J. Phys. Chem. A* **1997**, *101*, 9421–9429.
- (37) Gutbrod, R.; Schindler, R. N.; Kraka, E.; Cremer, D. Formation of OH Radicals in the Gas Phase ozonolysis of Alkenes: The Unexpected Role of Carbonyl Oxides. *Chem. Phys. Lett.* **1996**, *252*, 221–229.
- (38) Tajti, A.; Szalay, P. G.; Csanász, A. G.; Kallay, M.; Gauss, J.; Valeev, E. F.; Flowers, B. A.; Vazquez, J.; Stanton, J. F. HEAT: High Accuracy Extrapolated Ab Initio Thermochemistry. *J. Chem. Phys.* **2004**, *121*, 11599–11613.
- (39) Bomble, Y. J.; Vazquez, J.; Kallay, M.; Michauk, C.; Szalay, P. G.; Csanász, A. G.; Gauss, J.; Stanton, J. F. High-Accuracy Extrapolated Ab Initio Thermochemistry. II. Minor Improvements to the Protocol and a Vital Simplification. *J. Chem. Phys.* **2006**, *125*, 064108–8.
- (40) Harding, M. E.; Vazquez, J.; Ruscic, B.; Wilson, A. K.; Gauss, J.; Stanton, J. F. High-Accuracy Extrapolated Ab Initio Thermochemistry. III. Additional Improvements and Overview. *J. Chem. Phys.* **2008**, *128*, 114111–15.
- (41) Miller, W. H. Semi-Classical Theory for Non-Separable Systems: Construction of “Good” Action-Angle Variables for Reaction Rate Constants. *Faraday Discuss. Chem. Soc.* **1977**, *62*, 40–46.
- (42) Miller, W. H.; Hernandez, R.; Handy, N. C.; Jayatilaka, D.; Willets, A. Ab Initio Calculation of Anharmonic Constants for a Transition-State, with Application to Semiclassical Transition-State Tunneling Probabilities. *Chem. Phys. Lett.* **1990**, *172*, 62–68.
- (43) Hernandez, R.; Miller, W. H. Semi-Classical Transition State Theory. A New Perspective. *Chem. Phys. Lett.* **1993**, *214*, 129–136.
- (44) Nguyen, T. L.; Stanton, J. F.; Barker, J. R. A Practical Implementation of Semi-Classical Transition State Theory for Polyatomics. *Chem. Phys. Lett.* **2010**, *499*, 9–15.
- (45) Nguyen, T. L.; Stanton, J. F.; Barker, J. R. Ab Initio Reaction Rate Constants Computed Using Semiclassical Transition-State Theory:  $\text{HO} + \text{H}_2 = \text{H}_2\text{O} + \text{H}$  and Isotopologues. *J. Phys. Chem. A* **2011**, *115*, 5118–5126.
- (46) 2DME-SSS is a chemical kinetic program that solves a two-dimensional master-equation for gas-phase reactions in parallel using the Steady-State approach. It is developed, implemented, and maintained by T. L. Nguyen and J. F. Stanton, Department of Chemistry, The University of Texas at Austin, version June-2014. Nguyen, T. L.; Stanton, J. F. A Steady-State Approximation to the Two-Dimensional Master Equation for Chemical Kinetics Calculations. *J. Phys. Chem. A* **2015**, DOI: 10.1021/acs.jpca.5b00997.
- (47) Almlöf, J.; Taylor, P. R. General Contraction of Gaussian-Basis Sets. 1. Atomic Natural Orbitals for 1st-Row and 2nd-Row Atoms. *J. Chem. Phys.* **1987**, *86*, 4070–4077.
- (48) Almlöf, J.; Taylor, P. R. General Contraction of Gaussian-Basis Sets. 2. Atomic Natural Orbitals and the Calculation of Atomic and Molecular-Properties. *J. Chem. Phys.* **1990**, *92*, 551–560.
- (49) McCaslin, L. M.; Stanton, J. F. Calculation of Fundamental Frequencies for Small Polyatomic Molecules: A Comparison of Correlation-Consistent and Atomic Natural Orbital Basis Sets. *Mol. Phys.* **2013**, *111*, 1492–1496.
- (50) Mills, I. M. Vibration–Rotation Structure in Asymmetric- and Symmetric-Top Molecules. In *Molecular Spectroscopy: Modern Research*; Rao, K. N., Mathews, C. W., Eds.; Academic Press: New York, 1972; Vol. 1, p 115.
- (51) NIST Computational Chemistry Comparison and Benchmark Database, NIST Standard Reference Database Number 101, release 16a; Johnson, R. D., III, Ed.; <http://cccbdb.nist.gov/> (accessed February 20, 2015).
- (52) Stanton, J. F.; Gauss, J.; Harding, M. E.; Szalay, P. G.; Auer, w. c. f. A. A.; Bartlett, R. J.; Benedikt, U.; Berger, C.; Bernholdt, D. E.; Bomble, Y. J.; et al. CFOUR — Coupled-Cluster Techniques for Computational

Chemistry is a program package for performing high-level quantum chemical calculations on atoms and molecules, 2014, <http://www.cfour.de>.

(53) Kállay, M.; Rolik, Z.; Ladjánszki, L.; Szegedy, L.; Ladóczki, J.; Csontos, J.; Kornis, B. MRCC, A Quantum Chemical Program Suite. See Also Kállay, M.; Rolik, Z. A General-Order Local Coupled-Cluster Method Based on the Cluster-in-Molecule Approach. *J. Chem. Phys.* **2011**, *135*, 104111 as well as [Www.Mrcc.hu](http://www.Mrcc.hu). (accessed January 9, 2012).

(54) Ruscic, B.; Pinzon, R. E.; Morton, M. L.; von Laszewski, G.; Bittner, S. J.; Nijssure, S. G.; Amin, K. A.; Minkoff, M.; Wagner, A. F. Introduction to Active Thermochemical Tables: Several “Key” Enthalpies of Formation Revisited. *J. Phys. Chem. A* **2004**, *108*, 9979–9997.

(55) Ruscic, B.; Pinzon, R. E.; von Laszewski, G.; Kodeboyina, D.; Burcat, A.; Leahy, D.; Montoya, D.; Wagner, A. F. Active Thermochemical Tables: Thermochemistry for the 21st Century. *J. Phys. Conf. Ser.* **2005**, *16*, S61–S70.

(56) Ruscic, B. Updated Active Thermochemical Tables (ATcT) Values Based on ver. 1.112 of the Thermochemical Network (2014); available at [ATcT.anl.gov](http://ATcT.anl.gov).

(57) Karton, A.; Kettner, M.; Wild, D. A. Sneaking up on the Criegee Intermediate from Below: Predicted Photoelectron Spectrum of the  $\text{CH}_2\text{OO}^-$  anion and W3-F12 Electron Affinity of  $\text{CH}_2\text{OO}$ . *Chem. Phys. Lett.* **2013**, *585*, 15–20.

(58) Cremer, D.; Gauss, J.; Kraka, E.; Stanton, J. F.; Bartlett, R. A. CCSD(T) Investigation of Carbonyl Oxide and Dioxirane. Equilibrium Geometries, Dipole Moments, Infrared Spectra, Heats of Formation and Isomerization Energies. *J. Chem. Phys. Lett.* **1993**, *209*, 547–556.

(59) Lovas, F. J.; Suenram, R. D. Identification of Dioxirane ( $\text{H}_2\text{COO}$ ) in Ozone-Olefin Reactions via Microwave Spectroscopy. *Chem. Phys. Lett.* **1977**, *51*, 453–456.

(60) Martinez, R. I.; Hull, R. E.; Herron, J. T. Mass Spectrometric Detection of Dioxirane,  $\text{H}_2\text{COO}$ , and its Decomposition Products,  $\text{H}_2$  and CO, from the Reaction of Ozone with Ethylene. *Chem. Phys. Lett.* **1977**, *51*, 457–459.

(61) Fong, G. D.; Kuczkowski, R. L. Mechanism of the Ozonolysis of Ethylene in the Liquid Phase. *J. Am. Chem. Soc.* **1980**, *102*, 4763–4768.

(62) Schreiner, P. R.; Reisenauer, H. P. Spectroscopic Identification of Dihydroxycarbene. *Angew. Chem., Int. Ed.* **2008**, *47*, 7071–7074.

(63) Womack, C. C.; Crabtree, K. N.; McCaslin, L.; Martinez, O.; Field, R. W.; Stanton, J. F.; McCarthy, M. C. Gas-Phase Structure Determination of Dihydroxycarbene, One of the Smallest Stable Singlet Carbenes. *Angew. Chem., Int. Ed.* **2014**, *53*, 4089–4092.

(64) Chen, B. Z.; Anglada, J. M.; Huang, M. B.; Kong, F. The Reaction of  $\text{CH}_2(\text{X}^3\text{B}_1)$  with  $\text{O}_2(\text{X}^3\Sigma_g^-)$ : A Theoretical CASSCF/CASPT2 Investigation. *J. Phys. Chem. A* **2002**, *106*, 1877–1884.

(65) Wheeler, S. E.; Ess, D. H.; Houk, K. N. Thinking Out of the Black Box: Accurate Barrier Heights of 1,3-Dipolar Cycloadditions of Ozone with Acetylene and Ethylene. *J. Phys. Chem. A* **2008**, *112*, 1798–1807.

(66) Forst, W. *Theory of Unimolecular Reactions*; Academic Press: New York and London, 1973.

(67) Forst, W. *Unimolecular Reactions: A Concise Introduction*; Cambridge University Press: Cambridge, U.K., 2003.

(68) Holbrook, K. A.; Pilling, M. J.; Robertson, S. H. *Unimolecular Reactions*, 2nd ed.; John Wiley & Sons Ltd.: New York, NY, 1996.

(69) Frankcombe, T. J.; Smith, S. C.; Gates, K. E.; Robertson, S. H. A Master Equation Model for Bimolecular Reaction via Multi-Well Isomerizing Intermediates. *Phys. Chem. Chem. Phys.* **2000**, *2*, 793–803.

(70) Zhang, J.; Donahue, N. M. Constraining the Mechanism and Kinetics of  $\text{OH} + \text{NO}_2$  and  $\text{HO}_2 + \text{NO}$  Using the Multiple-Well Master Equation. *J. Phys. Chem. A* **2006**, *110*, 6898–6911.

(71) MultiWell-2014 Software. Designed and maintained by Barker, J. R. with contributors Ortiz, N. F.; Preses, J. M.; Lohr, L. L.; Maranzana, A.; Stimac, P. J.; Nguyen, T. L.; Dhillip-Kumar, T. J. University of Michigan, Ann Arbor, MI, 2014 <http://aoss.engin.umich.edu/multiwell/> (accessed March 19, 2014).

(72) Hippler, H.; Troe, J.; Wendelken, H. J. Collisional Deactivation of Vibrationally Highly Excited Polyatomic Molecules. II. Direct Observations for Excited Toluene. *J. Chem. Phys.* **1983**, *78*, 6709–6717.

(73) Nguyen, T. L.; Barker, J. R. Sums and Densities of Fully Coupled Anharmonic Vibrational States: A Comparison of Three Practical Methods. *J. Phys. Chem. A* **2010**, *114*, 3718–3730.

(74) Baer, T.; Hase, W. L. *Unimolecular Reaction Dynamics: Theory and Experiments*; Oxford University Press: New York-Oxford, 1996.

(75) Steinfeld, J. I.; Francisco, J. S.; Hase, W. L. *Chemical Kinetics and Dynamics*, 2 ed.; Prentice Hall International, Inc.: Upper Saddle River, NJ, 1999.

(76) Press, W. H.; Teukolsky, S. A.; Vetterling, W. T.; Flannery, B. P. *Numerical Recipes in Fortran 77: The Art of Scientific Computing*. Cambridge University Press: Cambridge, U.K., 1997.

(77) Wittig, C.; Nadler, I.; Reisler, H.; Noble, M.; Catanzarite, J.; Radhakrishnan, G. Nascent Product Excitations in Unimolecular Reactions: The Separate Statistical Ensembles Method. *J. Chem. Phys.* **1985**, *83*, S581–S588.

(78) Orlando, J. J.; Tyndall, G. S.; Bilde, M.; Ferronado, C.; Wallington, T. J.; Vereecken, L.; Peeters, J. Laboratory and Theoretical Study of the Oxy Radicals in the OH- and Cl-Initiated Oxidation of Ethene. *J. Phys. Chem. A* **1998**, *102*, 8116–8123.

(79) Vereecken, L.; Peeters, J. Theoretical Investigation of the Role of Intramolecular Hydrogen Bonding in  $\beta$ -Hydroxyethoxy and  $\beta$ -Hydroxyethylperoxy Radicals in the Tropospheric Oxidation of Ethene. *J. Phys. Chem. A* **1999**, *103*, 1768–1775.

(80) Vereecken, L.; Peeters, J.; Orlando, J. J.; Tyndall, G. S.; Ferronado, C. Decomposition of  $\beta$ -Hydroxypropoxy Radicals in the OH-Initiated Oxidation of Propene. A Theoretical and Experimental Study. *J. Phys. Chem. A* **1999**, *103*, 4693–4702.

(81) Orlando, J. J.; Tyndall, G. S.; Vereecken, L.; Peeters, J. The Atmospheric Chemistry of the Acetonyl Radical. *J. Phys. Chem. A* **2000**, *104*, 11578–11588.

(82) Baeza-Romero, M. T.; Glowacki, D. R.; Blitz, M. A.; Heard, D. E.; Pilling, M. J.; Rickard, A. R.; Seakins, P. W. A Combined Experimental and Theoretical Study of the Reaction between Methylglyoxal and OH/OD Radical: OH Regeneration. *Phys. Chem. Chem. Phys.* **2007**, *9*, 4114–4128.

(83) Nguyen, T. L.; Peeters, J.; Vereecken, L. Theoretical Study of the Gas-Phase Ozonolysis of  $\beta$ -Pinene ( $\text{C}_{10}\text{H}_{16}$ ). *Phys. Chem. Chem. Phys.* **2009**, *11*, S643–S656.

(84) Finlayson, B. J.; Pitts, J. N.; Atkinson, R. Low-Pressure Gas-Phase Ozone-Olefin Reactions. Chemiluminescence, Kinetics, and Mechanisms. *J. Am. Chem. Soc.* **1974**, *96*, S356–S367.

(85) Celani, P.; Stoll, H.; Werner, H. J.; Knowles, P. J. The CIPT2Method: Coupling of Multi-Reference Configuration Interaction and Multi-Reference Perturbation Theory. Application to the Chromium Dimer. *Mol. Phys.* **2004**, *102*, 2369–2379.

(86) Chao, W.; Hsieh, J. T.; Chang, C. H.; Lin, J. J. M. Direct Kinetic Measurement of the Reaction of the Simplest Criegee Intermediate with Water Vapor. *Science (Washington, DC, U.S.)* **2015**, *347*, 751–754.

(87) Okumura, M. Just Add Water Dimer. *Science (Washington, DC, U.S.)* **2015**, *347*, 718–719.

(88) Lewis, T. R.; Blitz, M. A.; Heard, D. E.; Seakins, P. W. Direct Evidence for a Substantive Reaction between the Criegee Intermediate,  $\text{CH}_2\text{OO}$ , and the Water Vapour Dimer. *Phys. Chem. Chem. Phys.* **2015**, *17*, 4859–4863.

(89) Ryzhkov, A. B.; Ariya, P. A. A Theoretical Study of the Reactions of Parent and Substituted Criegee Intermediates with Water and the Water Dimer. *Phys. Chem. Chem. Phys.* **2004**, *6*, S042–S050.

(90) Anglada, J. M.; Bofill, J. M.; Olivella, S.; Sole, A. Unimolecular Isomerizations and Oxygen Atom Loss in Formaldehyde and Acetaldehyde Carbonyl Oxides. A Theoretical Investigation. *J. Am. Chem. Soc.* **1996**, *118*, 4636–4647.